ABCG2 expression is related to low 5-ALA photodynamic diagnosis (PDD) efficacy and cancer stem cell phenotype, and suppression of ABCG2 improves the efficacy of PDD

Noriko Kawai[1,2], Yoshihiko Hirohashi[1] *, Yuma Ebihara[2], Takuma Saito[1,3], Aiko Murai[1], Takahiro Saito[2], Tomohide Shirosaki[2], Terufumi Kubo[1], Munehide Nakatsugawa[1], Takayuki Kanaseki[1], Tomohide Tsukahara[1], Toshiaki Shichinohe[2], Liming Li[3], Satoshi Hirano[2], Toshihiko Torigoe[1] *

1 Department of Pathology, Sapporo Medical University School of Medicine, Sapporo, Hokkaido, Japan,
2 Department of Gastroenterological Surgery II, Hokkaido University Graduate School of Medicine, Sapporo, Hokkaido, Japan, 3 Graduate School of Photonic Science, Chitose Institute for Science and Technology, Chitose, Hokkaido, Japan

* torigoe@sapmed.ac.jp (TT); hirohash@sapmed.ac.jp (YH)

🔓 OPEN ACCESS

Abstract

Photodynamic diagnosis/therapy (PDD/PDT) are novel modalities for the diagnosis and treatment of cancer. The photosensitizer protoporphyrin IX is metabolized from 5-aminolevulinic acid (5-ALA) intracellularly, and PDD/PDT using 5-ALA have been approved in dermatologic malignancies and gliomas. However, the molecular mechanism that defines the efficacy of PDD/PDT is unknown. In this study, we analyzed the functions of ATP-binding cassette (ABC) transporters in PDD using 5-ALA. Most of the human gastrointestinal cancer line cells examined showed a homogenous staining pattern with 5-ALA, except for the pancreatic cancer line PANC-1, which showed heterogeneous staining. To analyze this heterogeneous staining pattern, single cell clones were established from PANC-1 cells and the expression of ABC transporters was assessed. Among the ABC transporter genes examined, *ABCG2* showed an inverse correlation with the rate of 5-ALA-positive staining. PANC-1 clone #2 cells showed the highest level of *ABCG2* expression and the lowest level of 5-ALA staining, with only a 0.6% positive rate. Knockdown of the *ABCG2* gene by small interfering RNAs increased the positive rate of 5-ALA staining in PANC-1 wild-type and clone cells. Interestingly, PANC-1 clone #2 cells showed the high sphere-forming ability and tumor-formation ability, indicating that the cells contained high numbers of cancer stem cells (CSCs). Knockdown or inhibition of *ABCG2* increased the rate of 5-ALA staining, but did not decrease sphere-forming ability. These results indicate that gastrointestinal cancer cell lines expressing high levels of ABCG2 are enriched with CSCs and show low rates of 5-ALA staining, but 5-ALA staining rates can be improved by inhibition of ABCG2.

Introduction

Photodynamic diagnosis/therapy (PDD/PDT) are novel modalities to detect cancer cells based on the principle that a photosensitizer can accumulate specifically in cancer cells. Recently, PDD and PDT with 5-aminolevulinic acid (5-ALA) have been used for the diagnosis of glioma [1–4], and the application of PDD/PDT is expanding to various cancers. PDD is an especially useful approach for intraoperative cancer diagnosis, such as gastric cancer and pancreatic cancer, and can detect intraperitoneal lymph node metastasis or peritoneal metastasis because the presence of peritoneal dissemination or distant lymph node metastasis is critical for the surgical approach used, and the accessibility of pathological diagnosis using frozen sections is often limited.

The detection rate of PDD is essential for its successful application; however, its sensitivity is varied in various cancers and its detection rate is sometimes low and not satisfactory [5–8]. Thus, the identification of novel biomarkers for PDD and the improvement of the success rate of PDT are important. 5-ALA is transported into the cytoplasm by the amino acid transporters PEPT1 and PEPT2, and the intermediate coproporphyrinogen III is synthesized. Coproporphyrinogen III is transported from the cytoplasm to the mitochondria by the ATP-binding cassette (ABC) transporter ABCB6. In the mitochondria, the photosensitizer protoporphyrin IX (PpIX) is synthesized from coproporphyrinogen III. PpIX is exported by ABCG2 from the mitochondria to the cytoplasm and from the cytoplasm to the extracellular space [9]. Thus, several molecules are involved in the accumulation of PpIX, and several approaches have been tried to improve the efficacy of 5-ALA PDD/PDT [10, 11]. Recent studies have demonstrated that 5-ALA PDD is useful for the detection of lymph node metastasis and peritoneal dissemination, indicating that this approach can be a powerful tool during surgical treatment [6, 12].

Cancer stem cells (CSCs) are defined as small subpopulation of cancer cells that are endowed with high tumorigenicity, capacity for self-renewal, and differentiation ability [13], and CSCs are resistant to chemotherapy and radiotherapy due to several molecular mechanisms, namely, high expression of anti-apoptosis proteins, dormant state, and high expression of transporters [14, 15]. Therefore, an effective treatment for CSCs is essential to improve current cancer therapy.

In this study, we investigated the efficacy of 5-ALA PDD using gastrointestinal cancer cell lines. We found that the pancreatic cancer cell line PANC-1 showed lower PpIX accumulation than the other cell lines examined. Analysis at clone level revealed that high ABCG2 expression was responsible for the lower accumulation of PpIX. Furthermore, ABCG2-high clone cells were enriched with CSCs, and inhibition of ABCG2 improved 5-ALA PDD. Thus, ABCG2 might be a novel target to improve the detection and therapeutic efficacy of 5-ALA PDD/PDT for CSCs.

Materials and methods

Ethics statement

Mice were maintained and experimented on in accordance with the guidelines of and after approval by the Committee of Sapporo Medical University School of Medicine, Animal Experimentation Center under permit number (08–006). Any animal found unhealthy or sick was promptly euthanized.

Cell lines and culture methods

The human pancreas cancer cell lines CFPAC and PANC-1 (American Type Culture Collection, Rockville, MD) were cultured in Dulbecco's modified Eagle's medium (DMEM; Sigma-

Aldrich, St. Louis, MO) supplemented with 10% fetal bovine serum (FBS; Sigma-Aldrich) and 5% penicillin-streptomycin (5 mg/mL penicillin, 5 mg/mL streptomycin; Thermo Fisher Scientific, Waltham, MA). The gastric cancer cell line MKN45 (Japanese Collection of Research Bioresources Cell Bank, Osaka, Japan), esophagus cancer cell lines TE4 and TE9 (Japanese Cell Resource Center for Biomedical Research, Sendai, Japan), and pancreas cancer cell line PK9 (Cell Resource Center for Biomedical Research, Institute of Development, Aging and Cancer, Tohoku University, Sendai, Japan) were cultured in RPMI-1640 medium (Sigma-Aldrich) supplemented with 10% FBS and 5% penicillin-streptomycin.

5-ALA staining and fluorescence-activated cell sorting analysis

The cell lines were suspended at 1.0×10^6 cells/mL in DMEM supplemented with 5% FBS. 5-ALA (Novel Pharma, Tokyo, Japan) was added to the suspended cells at a final concentration of 150 μg/mL and incubated for 4 h at 37˚C. The cells were washed with 1× phosphate-buffered saline (PBS) twice and analyzed using a fluorescence-activated cell sorting (FACS) Aria II (BD Biosciences, San Jose, CA). PpIX fluorescence was detected at excitation and emission wavelengths of 488 nm laser with a 695/40 nm band-pass filter. 5-ALA non-treated cells were used as negative controls.

Percent mean fluorescent intensity (%MFI) increase was calculated by following formula: % MFI increase = (MFI of 5-ALA treated sample)*100/(MFI of 5-ALA non-treated sample)

Establishment of PANC-1 clone cells

PANC-1 cells were suspended at 1.0×10^6 cells/mL in DMEM supplemented with 5% FBS, stained with 5-ALA for 4 h at 37˚C, and sorted into single cells into 96-well plates using a FACS Aria II. After culture for several weeks, seven clone cell lines were established and used for further analysis.

RT-PCR and quantitative RT-PCR

Total RNA samples were extracted using an RNeasy Mini Kit (QIAGEN, Germantown, MD), and cDNA samples were synthesized with 1 μg total RNA using Superscript III Reverse Transcriptase (Thermo Fisher Scientific) in accordance with the manufacturer's protocol. PCR was performed using Taq DNA polymerase (QIAGEN) and the following thermal cycling conditions: initial denaturation for 2 min at 94˚C, followed by 35 cycles of denaturation for 15 s at 94˚C, annealing for 30 s at 55˚C, and elongation for 30 s at 72˚C, and a final elongation step for 5 min at 72˚C. The primer pairs used for RT-PCR analysis are in S1 Table and previous reports [16, 17].

Quantitative RT-PCR (qRT-PCR) was performed using an ABI PRISM 7000 Sequence Detection System (Thermo Fisher Scientific) in accordance with the manufacturer's protocol. The *ABCG2* probe was designed by the manufacturer (TaqMan Gene expression assays; Thermo Fisher Scientific), and thermal cycling was performed under the following conditions: 45 cycles of 95˚C for 15 s and 60˚C for 1 min. Each experiment was performed in triplicate, and *GAPDH* was used for internal normalization.

Small interfering RNA transfection and treatment with an ABCG2 inhibitor

Pre-designed small interfering RNAs (siRNAs) targeting *ABCG2* were purchased (Silencer Select siRNA; s18056, s18057, s18058) from Thermo Fisher Scientific, and siRNA transfection was performed using the Lipofectamine RNAiMAX reagent (Thermo Fisher

Scientific) in accordance with the manufacturer's protocol. The cells were seeded in 6-well plates at 3.0×10^5 cells/well in 2 mL DMEM supplemented with 10% FBS and 5% penicillin-streptomycin. Negative control siRNA (Silencer Select) was used as a negative control. Cells transfected with 20 nM siRNAs were harvested at 2 days after transfection and used for some experiments.

Ko143 (Santa Cruz Biotechnology, Dallas, TX), an ABCG2 inhibitor, was used at a concentration of 10 or 20 μM for 24 h.

Side population assay, sphere-forming assay and Mouse xenograft assay

Side population (SP) and sphere-forming assays were performed as described previously [18, 19]. Briefly, PANC-1 wild-type (W/T) cells, clone #2 cells, and clone #4 cells were stained with Hoechst 33342 (Lonza, Basel, Switzerland) at a final concentration of 2.5 μg/mL for 60 min at 37°C. After washing with PBS, the cells were analyzed using a FACS Aria II. Verapamil was used at 75 μM as a negative control.

For the sphere-forming assay, the cells were seeded into a 96-well Ultra-Low Attachment Surface Culture Plate (Corning) at 1, 10, 100, and 1000 cells/wells in DMEM/F12 medium supplemented with 20 ng/mL basic fibroblast growth factor (R&D Systems, Minneapolis, MN, USA) and 20 ng/mL epidermal growth factor (R&D Systems) for 7 days. The sphere-positive wells were counted, and CSC frequency and statistical analysis were performed at the ELDA web site (http://bioinf.wehi.edu.au/software/elda) [20].

Xenograft transplantation experiments using animals were performed in accordance with the institutional guidelines for the use of laboratory animals. PANC-1 clone #2 and clone #4 cells were suspended at 1000 or 10000 cells in 100 μl PBS mixed with Matrigel (BD) at a 1:1 volume and injected subcutaneously into the backs of 4-6-week-old female BALB/c-nu/nu mice. Tumor size was assessed weekly using a caliper and calculated using following formula: tumor size (mm^3) = (longest diameter × shortest diameter^2)/2.

Statistical analysis

Student's *t*-test was used to compare two groups. P<0.05 was considered significant difference. Correlation between expressions of *ABCG2* and %MFI increase was analyzed by Pearson's correlation coefficient.

Results

The pancreatic cancer cell PANC-1 shows heterogeneous 5-ALA staining

PDD based on 5-ALA-induced PpIX has been applied to several malignancies based on safety and specificity; however, the molecular aspects that define the efficacy of PDD are unknown. In this study, we analyzed several gastrointestinal cancer cell lines to investigate differences in PpIX accumulation. Although most of the TE4, TE9, MKN45, CFPAC, and PK9 cells showed high PpIX intensity with a positive rate of almost 100%, PANC-1 cells showed lower PpIX intensity with a positive rate of 43.2% (Fig 1A). To analyze in detail, %MFI increase was calculated, and PANC-1 cells showed also the lowest %MFI increase (Fig 1B).

Single cell analysis reveals clonal variation for 5-ALA staining

Since PANC-1 cells showed heterogeneous 5-ALA staining pattern, we established PANC-1 clone cells to analyze the heterogeneity of PpIX accumulation at the single cell level (Fig 2A). PANC-1 clone cells were stained with 5-ALA and the accumulation of PpIX was analyzed flow cytometry. The results revealed a heterogeneous PpIX accumulation pattern between the
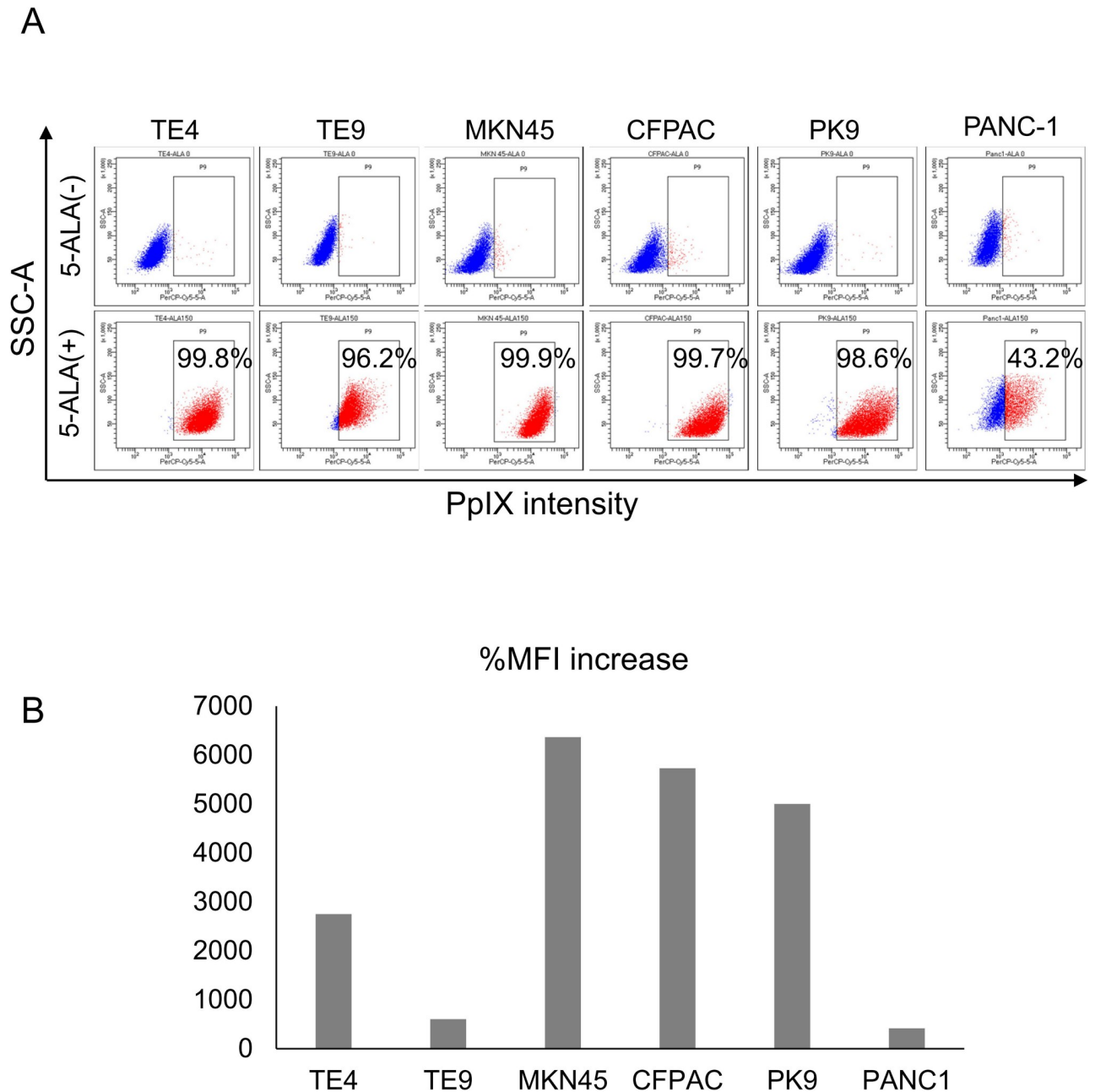
A

B

Fig 1. 5-ALA staining of gastrointestinal cancer cells. (A) FACS analysis of 5-ALA-stained gastrointestinal cancer cells. Esophageal cancer cells (TE4 and TE9), gastric cancer cells (MKN45), and pancreatic cancer cells (CFPAC, PANC-1, and PK9) were stained with 5-ALA (150 μg/mL) for 4 h and analyzed by flow cytometry. Non-stained cells were used as negative controls. Percentages indicate the positive rates of PpIX intensity. **(B) Summary of percent mean fluorescent increase (%MFI).**

PANC-1 clone cells (Fig 2B). Clone #2 cells showed only a 0.6% positive rate, whereas clones #3 and #4 showed a greater than 50% positive rate, which was higher than that observed in W/T PANC-1 cells. These data indicate that 5-ALA staining was heterogeneous, and it was difficult to detect PpIX accumulation in some PANC-1 clone cells. Clone #2 cells showed the lowest %MFI increase as well (Fig 2C).
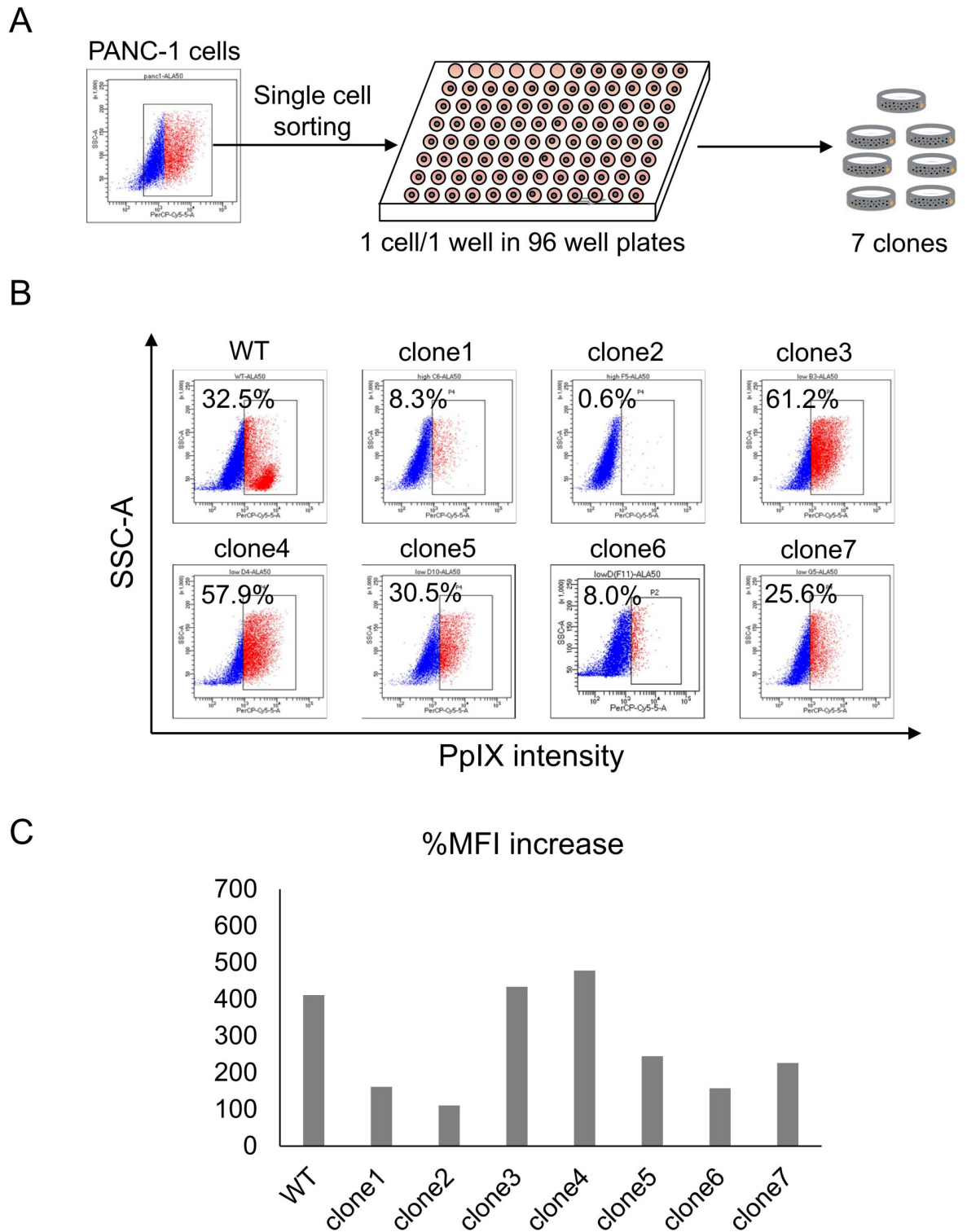
Fig 2. Establishment of PANC-1 clone cells. (A) Schematic summary of single cell sorting of PANC-1 cells. (B) FACS analysis of 5-ALA-stained PANC-1 clone cells. Non-stained cells were used as negative controls. Percentages indicate the positive rates of PpIX intensity. **(C) Summary of percent mean fluorescent increase (%MFI).**

Gene screening reveals that ABCG2 is a candidate for low-5-ALA staining

To elucidate the mechanism underlying the heterogeneous 5-ALA staining, we focused on transporters that are responsible for 5-ALA uptake and PpIX efflux. Previous studies revealed that oligopeptide transporters PEPT1 and PEPT2 are responsible for 5-ALA uptake [21–23]. Thus, we analyzed the expression of *PEPT1* and *PEPT2* by RT-PCR; however, there was no significant difference in their expression between the PANC-1 clone cells (Fig 3B). We then analyzed ABC transporters using ABC transporter gene-specific primers, because ABC transporters are related to 5-ALA uptake and PpIX efflux (Fig 3A). ABCB6 is responsible for 5-ALA uptake, while ABCG2 is responsible for PpIX efflux [24, 25]. However, the expression of *ABCB6* was equivalent between W/T PANC-1 cells and clones #2, #4, and #6. *ABCG2* expression was high in PANC-1 clone #2 cells and low in clone #4 cells. No other ABC transporter genes showed a significant difference in their expression between the PANC-1 clone cells. Therefore, we focused on the *ABCG2* gene. Genes related to accumulation of PpIX including *PEPT1*, *PEPT2*, *ABCB6* and *ABCG2* expression were analyzed in other cell lines (Fig 3B). PANC-1, TE4 and TE9 cells expressed ABCG2, but MKN45 and CFPAC cells did not. MKN45 and CFPAC cells express PEPT1 at high levels, but other cell lines barely expressed *PEPT1* and *PEPT2*. To confirm the expression of *ABCG2*, we performed qRT-PCR and found that PANC-1 clone #2 cells showed the highest level of *ABCG2* expression, whereas clones #4 and #5 showed the lowest expression levels (Fig 3C). These data indicate an inverse correlation between the expression level of the *ABCG2* gene and PpIX-positive rates.

To analyze the relation of quantitative *ABCG2* expression and %MFI increase correlation coefficient (CI) was calculated. The expressions of *ABCG2* in cancer cell lines and %MFI increase showed statistically significant inverse correlation (r = -0.9388, p = 0.0055) (Fig 3D). The expressions of *ABCG2* in PANC-1 clone cells and %MFI increase showed tendency to inverse correlation but did not reach statistical significance (r = -0.4558, p = 0.2563) (Fig 3E). All these data suggest the inverse relation of *ABCG2* expression and PpIX intensity.

ABCG2 knockdown using siRNAs reveals that ABCG2 has a role in low 5-ALA staining

A previous study revealed that ABCG2 has a role in PpIX efflux [24]; thus, we analyzed the role of ABCG2 in 5-ALA staining using siRNAs. The *ABCG2* gene was knocked down using *ABCG2*-specific siRNAs in PANC-1 W/T, clone #2 cells, and clone #4 cells, and knockdown efficiency was confirmed by qRT-PCR (Fig 4A). Knockdown of *ABCG2* increased PpIX-positive rates in W/T cells, clone #2 cells, and clone #4 cells (Fig 4B), indicating that ABCG2 has a role in low 5-ALA staining rates.

ABCG2-high cells are enriched with CSCs, but ABCG2 is not related to cancer stemness

Several studies have revealed that a highly tumorigenic subpopulation, termed CSCs, are enriched in SP cells, and SP cells are defined by ABCG2 expression [18, 26–29]. Therefore, we hypothesized that PANC-1 clone #2 cells are enriched with CSCs and performed an SP assay and sphere formation assay. PANC-1 clone #2 cells showed an SP rate of 15.9%, whereas W/T cells and clone #4 cells showed SP rates of 4.4% and 0.5%, respectively (Fig 5A). A sphere formation assay revealed that PANC-1 clone #2 cells has higher sphere formation ability than clone #4 cells (P = 0.0204) (Fig 5B). To analyze the expressions of stem cell genes in PANC-1 clone cells, we performed RT-PCR. Clone #2 cells showed relative high expression of *NANOG*, but clone #4 cells did not (Fig 3A). Clone #2 cells showed higher *CDH2* gene, an epithelial-
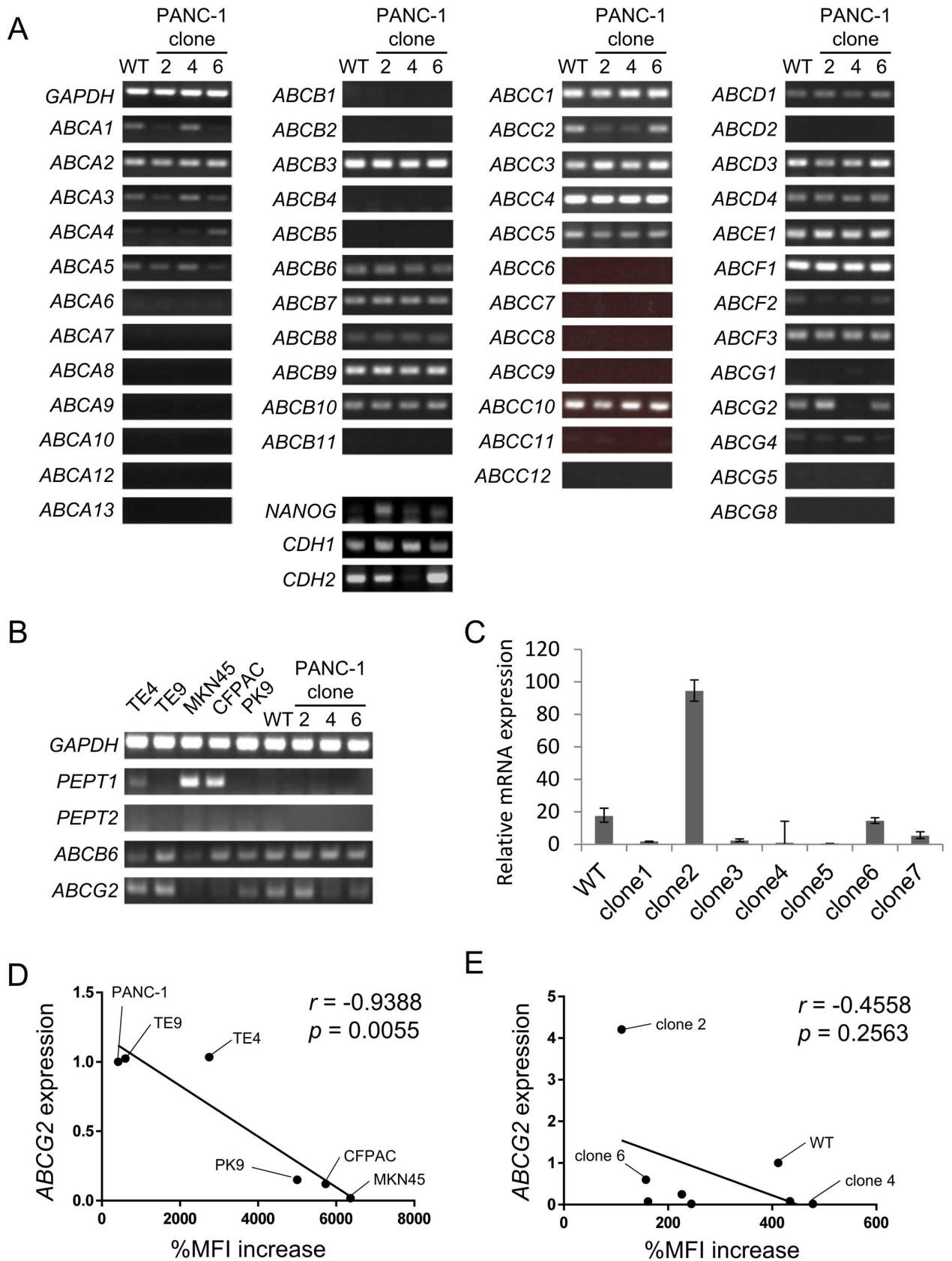
Fig 3. Expression of ABC transporter genes. (A) RT-PCR analysis of PANC-1 clone cells. The expression of ABC transporter genes, *NANOG*, *CDH1* and *CDH2* in PANC-1 W/T cells, clone #2 cells, clone #4 cells, and clone #6 cells was analyzed by RT-PCR. GAPDH was used as an internal positive control. **(B) RT-PCR analysis of gastrointestinal cancer cells.** *PEPT1*, *PEPT2*, *ABCB6* and *ABCG2* expression was analyzed by RT-PCR. GAPDH was used as an internal positive control. **(C) qRT-PCR analysis of *ABCG2* expression.** *ABCG2* expression was analyzed by qRT-PCR. Data are shown as the mean ± standard deviation. **(D) Correlation of expressions of *ABCG2* and %MFI increase.** Correlation of expression of quantitative ABCG2 expressions of gastrointestinal cancer cell lines and %MFI increase was analyzed by Pearson's correlation coefficient. **(E) Correlation of expressions of *ABCG2* and %MFI increase.** Correlation of expression of quantitative ABCG2 expressions of PANC-1 clone cells and %MFI increase was analyzed by Pearson's correlation coefficient.

mesenchymal transition marker than that in clone #4 cells suggesting that clone #2 cells are enriched with CSCs and have EMT-like phenotype (Fig 3A). Furthermore, clone #2 cells showed higher tumorigenicity than clone #4 cells (Fig 5C and 5D), indicating that clone #2 cells contain a higher proportion of CSCs compared with W/T or clone #4 cells. Since PANC-1 clone #2 cells showed the highest level of ABCG2 expression, we analyzed the relationship between ABCG2 expression and CSC phenotype. Knockdown of *ABCG2* using siRNAs and inhibition of ABCG2 using Ko143 decreased the SP rate (Fig 5E and 5F), whereas knockdown of *ABCG2* and inhibition of ABCG2 did not decrease sphere formation (Fig 5G and 5H), indicating that ABCG2 expression is not related to tumor formation.

Discussion

5-ALA PDD/PDT have been approved for dermatologic malignancies and gliomas and have been applied to several malignant tumors [30]. A phase III clinical trial of surgery with 5-ALA PDD for malignant gliomas revealed that it significantly improved progression-free survival [2], indicating that 5-ALA PDD is an effective approach for the diagnosis of malignant tumors. However, most of the patients enrolled in that study showed disease progression,
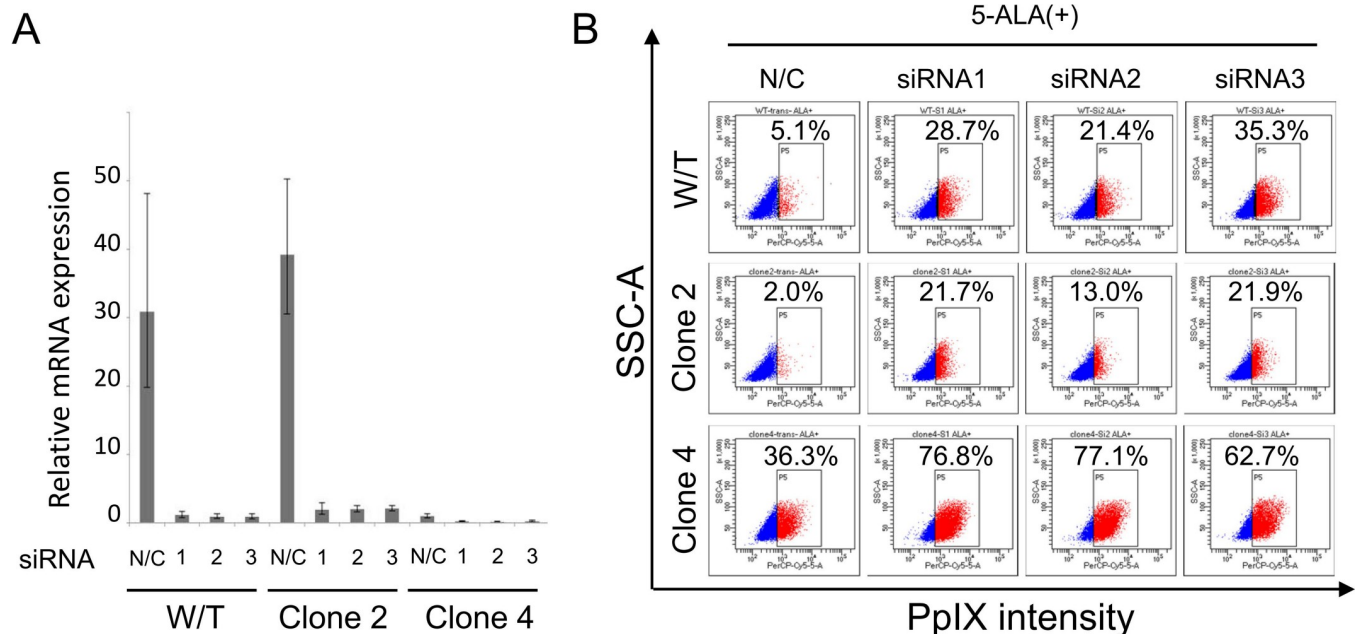
Fig 4. Knockdown of ABCG2 in PANC-1 clone cells increases 5-ALA staining. (A) qRT-PCR analysis of *ABCG2* expression. PANC-1 W/T cells, clone #2 cells, and clone #4 cells were transfected with ABCG2 siRNAs. At 2 days after transfection, *ABCG2* expression was analyzed by qRT-PCR. Data are shown as the mean ± standard deviation. **(B) FACS analysis of 5-ALA-stained ABCG2 knockdown cells.** PANC-1 W/T cells, clone #2 cells, and clone #4 cells were transfected with ABCG2 siRNAs. At 2 days after transfection, the cells were stained with 5-ALA (150 μg/mL) for 4 h and analyzed by flow cytometry. Percentages indicate the positive rates of PpIX intensity.

A
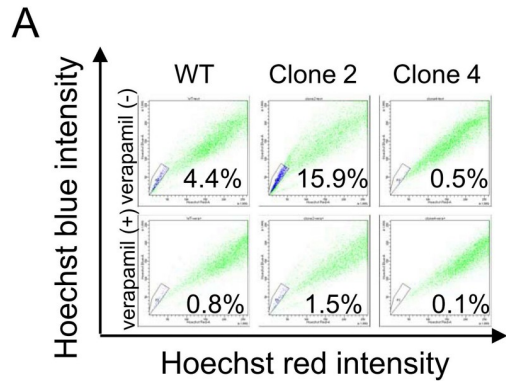
B

Sphere formation

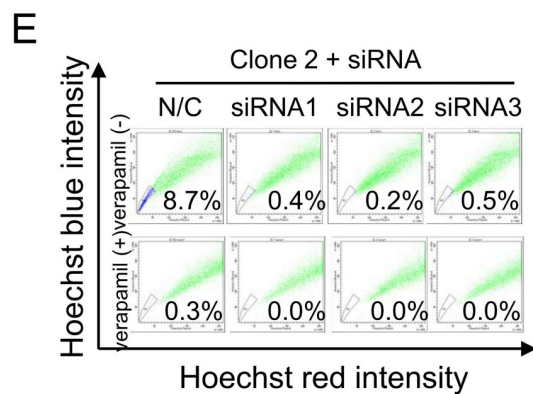| clones	Cells/well				CSC frequency	95% CI
	10^0	10^1	10^2	10^3		
W/T	0//24	0/24	24/24	24/24	1/43.8	28.3-67.9
Clone 2	0/24	4/24	24/24	24/24	1/32.8	20.8-51.8
Clone 4	0/24	0/24	20/24	24/24	1/72.5	46.3-113.7

*P=0.0204

C

D

E
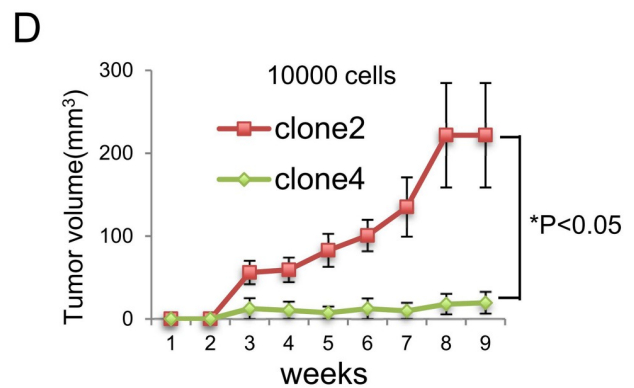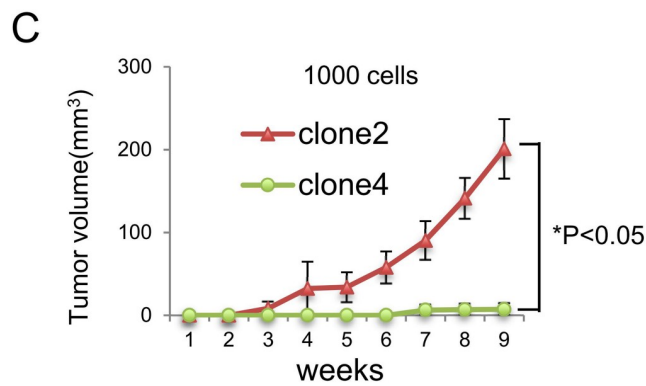
F

Sphere formation

siRNAs	Cells/well				CSC frequency	95% CI
	10^0	10^1	10^2	10^3		
N/C	0/24	0/24	4/24	24/24	1/325.1	205.2-515.2
siRNA1	0/24	0/24	12/24	24/24	1/163.1	97.2-274.1
siRNA2	0/24	0/24	2/24	24/24	1/376.6	240.5-589.9
siRNA3	0/24	0/24	6/24	24/24	1/278.6	173.1-448.8

*N.S.

G
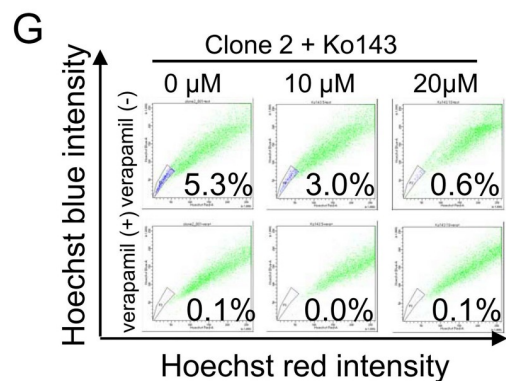
H

Sphere formation

Ko143	Cells/well				CSC frequency	95% CI
	10^0	10^1	10^2	10^3		
0 μM	0//24	10/24	24/24	24/24	1/20.0	12.2-33.2
10 μM	1/24	11/24	24/24	24/24	1/17.0	10.3-28.3
20 μM	0/24	3/24	24/24	24/24	1/35.3	22.6-55.4

*N.S.

Fig 5. Inhibition of ABCG2 decreases SP cells, but not sphere-forming ability. (A) SP analysis of PANC-1 cells. PANC-1 W/T cells, clone #2 cells, and clone #4 cells were stained with Hoechst 33342 and analyzed by flow cytometry. Verapamil was used as a negative control. Percentages indicate the rates of SP cells. **(B) Sphere-forming ability of PANC-1 cells.** PANC-1 W/T cells, clone #2 cells, and clone #4 cells were seeded in 96-well ultra-low attachment plates at 1, 10, 100, and 1000 cells/well. At 1 week later, sphere-forming wells were counted, and CSC frequency was calculated using the ELDA website. The chi-square test was performed to determine statistically significant differences. **(C and D) Tumorigenicity of PANC-1 clone #2 and #4 cells.** Growth curves of tumors derived from PANC-1 clone #2 and clone #4 cells. 1000 cells (C) and 10000 cells (D) were injected into BALB/c-nu/nu mice, and tumors were measured weekly. Data are shown as means±SD. Asterisks indicates a statistically difference (P<0.05). **(E) SP analysis of ABCG2 knockdown PANC-1 clone #2 cells.** PANC-1 clone #2 cells were transfected with ABCG2 siRNAs. At 2 days after transfection, the cells were analyzed by an SP assay. Verapamil was used as a negative control. Percentages indicate the rates of SP cells. **(F) Sphere-forming ability of ABCG2 knockdown PANC-1 clone #2 cells.** PANC-1 clone #2 cells were transfected with ABCG2 siRNAs. At 1 day after transfection, the cells were seeded in 96-well ultra-low attachment plates at 1, 10, 100, and 1000 cells/well. At 1 week later, sphere-forming wells were counted, and CSC frequency was calculated using the ELDA website. The chi-square test was performed to determine statistically significant differences. N.S.: No significant difference. **(G) SP analysis of Ko143-treated PANC-1 clone #2 cells.** PANC-1 clone #2 cells were treated with Ko143 at a concentration of 0, 10, or 20 μM for 24 h and analyzed by an SP assay. Verapamil was used as a negative control. Percentages indicate the rates of SP cells. **(H) Sphere-forming ability of Ko143-treated PANC-1 clone #2 cells.** PANC-1 clone #2 cells were seeded in 96-well ultra-low attachment plates at 1, 10, 100, and 1000 cells/well with Ko143 at a concentration of 0, 10, or 20 μM. At 1 week later, sphere-forming wells were counted, and CSC frequency was calculated using the ELDA website. The chi-square test was performed to determine statistically significant differences. N.S.: No significant difference.

demonstrating that detection efficacy needs to be improved. In this regard, several analyses at the molecular level have been reported.

ABCG2 (breast cancer resistance protein, BCRP) transports various endogenous and exogenous chemicals [31], thereby mediating drug resistance and affecting the pharmacological action of many compounds in different drug-resistant cancer cells [32–34]. A study using diffuse large B cell lymphoma cells revealed that ABCG2 is a transcriptional target of the hedgehog signaling transcription factor GLI1 [35]. Sonic hedgehog (SHH) signaling is one of the major signaling pathway activated in pancreatic cancer [36]. A phase Ib/II clinical trial using Vismodegib, an SHH inhibitor, plus gemcitabine did not improve progression-free or overall survival in patients with metastatic pancreatic cancer [37], suggesting difficulties in targeting SHH signaling. Regarding hedgehog signaling, a study using PANC-1 cells revealed that sphere-forming CSCs showed high expression of the epithelial-mesenchymal transition transcription factor SNAI1 and hedgehog signaling ligand SMO [38], indicating that the activation of SHH signaling, CSC phenotype, and epithelial-mesenchymal transition are deeply related to each other. In the present study, ABCG2-high PANC-1 clone #2 cells showed high sphere-forming ability compared with ABCG2-low clone #4 cells. Therefore, ABCG2-high pancreatic CSCs might be well targeted by 5-ALA PDT using an ABCG2 inhibitor, and this approach could be another way to target SHH signaling-activated pancreatic cancer cells. ABCG2 knockdown using siRNAs increased accumulation of PpIX, however, the PpIX positive rate did not reached 100% even in clone #4 cells. PANC-1 cells express both ABCB6 and ABCG2, however the expression levels of PEPT1 and PEPT2 were very low (Fig 3B). Therefore, the accumulation rates of PpIX in PANC-1 clone cells might also depend on also low expressions of PEPT1 and PEPT2. A recent study revealed that C6 rat glioma cells with low PpIX accumulation are enriched with glioma stem cells [39]. Interestingly, the accumulation of PpIX in glioma stem cells was not enhanced by ABCG2 inhibition using reserpine, but was enhanced by deferoxamine-mediated iron chelation, suggesting that PpIX accumulation depends on several factors.

ABCB6 is a transporter for the uptake of 5-ALA, and high ABCB6 expression is related to high PpIX accumulation [25]. High ABCB6 expression is related to the response to neoadjuvant chemotherapy in breast cancer and the progression of prostate cancer [40, 41]. Although, the molecular mechanisms by which ABCB6 expression is related to chemotherapy resistance or cancer progression are unknown, ABCB6-high malignant cancers are considered to be suitable targets for 5-ALA PDD/PDT because ABCB6-high cancer cells are thought to accumulate PpIX. However, the expression levels of ABCB6 were equivalent between PANC-1 W/T cells and clone cells by RT-PCR, and ABCB6 expression might not be related to PpIX accumulation

in pancreatic cancer cells. These results suggest that ABCB6 expression might not be an accurate marker for predicting the efficacy of 5-ALA PDD/PDT in pancreatic cancer. The accumulation of data using clinical samples from subjects with pancreatic cancer should be conducted in the future.

In summary, we reported that most of the gastrointestinal cancer cell lines examined showed homogenous 5-ALA staining. However, the pancreatic cancer cell line PANC-1 showed heterogeneous 5-ALA staining. High ABCG2 expression might be responsible for low 5-ALA staining, and CSCs are enriched in the ABCG2-high population. Inhibition of ABCG2 improved 5-ALA staining, but had no effect on cancer stemness. These results indicate that ABCG2 expression might become a novel biomarker for poor 5-ALA PDD/PDT efficacy, and the combination of 5-ALA PDD/PDT with an ABCG2 inhibitor might improve efficacy. Finally, CSCs could also be targeted by the combination of 5-ALA PDD/PDT with an ABCG2 inhibitor.

Supporting information

S1 Table. Information of RT-PCR primers.
(XLSX)

Acknowledgments

We thank J. Yanagawa for technical assistance.

Author Contributions

Conceptualization: Noriko Kawai, Yoshihiko Hirohashi, Yuma Ebihara, Terufumi Kubo, Munehide Nakatsugawa, Takayuki Kanaseki, Tomohide Tsukahara, Toshiaki Shichinohe, Liming Li, Satoshi Hirano, Toshihiko Torigoe.

Data curation: Noriko Kawai, Takuma Saito, Aiko Murai, Takahiro Saito, Tomohide Shirosaki.

Formal analysis: Noriko Kawai, Toshihiko Torigoe.

Funding acquisition: Toshihiko Torigoe.

Investigation: Noriko Kawai.

Methodology: Noriko Kawai.

Supervision: Yoshihiko Hirohashi, Yuma Ebihara, Toshiaki Shichinohe, Liming Li, Satoshi Hirano, Toshihiko Torigoe.

Writing – original draft: Noriko Kawai, Yoshihiko Hirohashi.

Writing – review & editing: Noriko Kawai, Yoshihiko Hirohashi, Yuma Ebihara, Satoshi Hirano, Toshihiko Torigoe.

References

1. Olzowy B, Hundt CS, Stocker S, Bise K, Reulen HJ, Stummer W. Photoirradiation therapy of experimental malignant glioma with 5-aminolevulinic acid. Journal of neurosurgery. 2002; 97(4):970–6. Epub 2002/10/31. https://doi.org/10.3171/jns.2002.97.4.0970 PMID: 12405389.

2. Stummer W, Pichlmeier U, Meinel T, Wiestler OD, Zanella F, Reulen HJ, et al. Fluorescence-guided surgery with 5-aminolevulinic acid for resection of malignant glioma: a randomised controlled multicentre phase III trial. The lancet oncology. 2006; 7(5):392–401. Epub 2006/05/02. https://doi.org/10.1016/S1470-2045(06)70665-9 PMID: 16648043.

3. Beck TJ, Kreth FW, Beyer W, Mehrkens JH, Obermeier A, Stepp H, et al. Interstitial photodynamic therapy of nonresectable malignant glioma recurrences using 5-aminolevulinic acid induced protoporphyrin IX. Lasers in surgery and medicine. 2007; 39(5):386–93. Epub 2007/06/15. https://doi.org/10.1002/lsm.20507 PMID: 17565715.

4. Stummer W, Beck T, Beyer W, Mehrkens JH, Obermeier A, Etminan N, et al. Long-sustaining response in a patient with non-resectable, distant recurrence of glioblastoma multiforme treated by interstitial photodynamic therapy using 5-ALA: case report. Journal of neuro-oncology. 2008; 87(1):103–9. Epub 2007/11/24. https://doi.org/10.1007/s11060-007-9497-x PMID: 18034212.

5. Loning M, Diddens H, Kupker W, Diedrich K, Huttmann G. Laparoscopic fluorescence detection of ovarian carcinoma metastases using 5-aminolevulinic acid-induced protoporphyrin IX. Cancer. 2004; 100 (8):1650–6. Epub 2004/04/10. https://doi.org/10.1002/cncr.20155 PMID: 15073853.

6. Murayama Y, Ichikawa D, Koizumi N, Komatsu S, Shiozaki A, Kuriu Y, et al. Staging fluorescence laparoscopy for gastric cancer by using 5-aminolevulinic acid. Anticancer research. 2012; 32(12):5421–7. Epub 2012/12/12. PMID: 23225446.

7. Liu Y, Endo Y, Fujita T, Ishibashi H, Nishioka T, Canbay E, et al. Cytoreductive surgery under aminolevulinic acid-mediated photodynamic diagnosis plus hyperthermic intraperitoneal chemotherapy in patients with peritoneal carcinomatosis from ovarian cancer and primary peritoneal carcinoma: results of a phase I trial. Annals of surgical oncology. 2014; 21(13):4256–62. Epub 2014/07/25. https://doi.org/10.1245/s10434-014-3901-5 PMID: 25056850; PubMed Central PMCID: PMC4218977.

8. Hillemanns P, Wimberger P, Reif J, Stepp H, Klapdor R. Photodynamic diagnosis with 5-aminolevulinic acid for intraoperative detection of peritoneal metastases of ovarian cancer: A feasibility and dose finding study. Lasers in surgery and medicine. 2017; 49(2):169–76. Epub 2016/11/20. https://doi.org/10.1002/lsm.22613 PMID: 27859395.

9. Koizumi N, Harada Y, Minamikawa T, Tanaka H, Otsuji E, Takamatsu T. Recent advances in photodynamic diagnosis of gastric cancer using 5-aminolevulinic acid. World journal of gastroenterology: WJG. 2016; 22(3):1289–96. Epub 2016/01/27. https://doi.org/10.3748/wjg.v22.i3.1289 PMID: 26811665; PubMed Central PMCID: PMC4716038.

10. Palasuberniam P, Yang X, Kraus D, Jones P, Myers KA, Chen B. ABCG2 transporter inhibitor restores the sensitivity of triple negative breast cancer cells to aminolevulinic acid-mediated photodynamic therapy. Scientific reports. 2015; 5:13298. Epub 2015/08/19. https://doi.org/10.1038/srep13298 PMID: 26282350; PubMed Central PMCID: PMC4539603.

11. Kim JH, Park JM, Roh YJ, Kim IW, Hasan T, Choi MG. Enhanced efficacy of photodynamic therapy by inhibiting ABCG2 in colon cancers. BMC Cancer. 2015; 15:504. Epub 2015/07/08. https://doi.org/10.1186/s12885-015-1514-4 PMID: 26149077; PubMed Central PMCID: PMC4494642.

12. Yonemura Y, Endo Y, Canbay E, Liu Y, Ishibashi H, Mizumoto A, et al. Photodynamic Detection of Peritoneal Metastases Using 5-Aminolevulinic Acid (ALA). Cancers. 2017; 9(3). Epub 2017/03/04. https://doi.org/10.3390/cancers9030023 PMID: 28257041; PubMed Central PMCID: PMC5366818.

13. Clarke MF, Dick JE, Dirks PB, Eaves CJ, Jamieson CH, Jones DL, et al. Cancer stem cells—perspectives on current status and future directions: AACR Workshop on cancer stem cells. Cancer research. 2006; 66(19):9339–44. Epub 2006/09/23. https://doi.org/10.1158/0008-5472.CAN-06-3126 PMID: 16990346.

14. Park CY, Tseng D, Weissman IL. Cancer stem cell-directed therapies: recent data from the laboratory and clinic. Molecular therapy: the journal of the American Society of Gene Therapy. 2009; 17(2):219–30. Epub 2008/12/11. https://doi.org/10.1038/mt.2008.254 PMID: 19066601; PubMed Central PMCID: PMC2835048.

15. Hirohashi Y, Torigoe T, Tsukahara T, Kanaseki T, Kochin V, Sato N. Immune responses to human cancer stem-like cells/cancer-initiating cells. Cancer science. 2016; 107(1):12–7. Epub 2015/10/07. https://doi.org/10.1111/cas.12830 PMID: 26440127; PubMed Central PMCID: PMC4724814.

16. Nishizawa S, Hirohashi Y, Torigoe T, Takahashi A, Tamura Y, Mori T, et al. HSP DNAJB8 Controls Tumor-Initiating Ability in Renal Cancer Stem-like Cells. Cancer research. 2012; 72(11):2844–54. Epub 2012/05/04. https://doi.org/10.1158/0008-5472.CAN-11-3062 PMID: 22552285.

17. Yasuda K, Torigoe T, Mariya T, Asano T, Kuroda T, Matsuzaki J, et al. Fibroblasts induce expression of FGF4 in ovarian cancer stem-like cells/cancer-initiating cells and upregulate their tumor initiation capacity. Laboratory investigation; a journal of technical methods and pathology. 2014. Epub 2014/10/21. https://doi.org/10.1038/labinvest.2014.122 PMID: 25329002.

18. Nakatsugawa M, Takahashi A, Hirohashi Y, Torigoe T, Inoda S, Murase M, et al. SOX2 is overexpressed in stem-like cells of human lung adenocarcinoma and augments the tumorigenicity. Laboratory investigation; a journal of technical methods and pathology. 2011; 91(12):1796–804. Epub 2011/09/21. https://doi.org/10.1038/labinvest.2011.140 PMID: 21931300.

19. Yasuda K, Hirohashi Y, Mariya T, Murai A, Tabuchi Y, Kuroda T, et al. Phosphorylation of HSF1 at serine 326 residue is related to the maintenance of gynecologic cancer stem cells through expression of HSP27. Oncotarget. 2017; 8(19):31540–53. Epub 2017/04/19. https://doi.org/10.18632/oncotarget.16361 PMID: 28415561; PubMed Central PMCID: PMC5458228.

20. Hu Y, Smyth GK. ELDA: extreme limiting dilution analysis for comparing depleted and enriched populations in stem cell and other assays. J Immunol Methods. 2009; 347(1–2):70–8. Epub 2009/07/02. https://doi.org/10.1016/j.jim.2009.06.008 PMID: 19567251.

21. Doring F, Walter J, Will J, Focking M, Boll M, Amasheh S, et al. Delta-aminolevulinic acid transport by intestinal and renal peptide transporters and its physiological and clinical implications. The Journal of clinical investigation. 1998; 101(12):2761–7. Epub 1998/06/24. https://doi.org/10.1172/JCI1909 PMID: 9637710; PubMed Central PMCID: PMC508867.

22. Rud E, Gederaas O, Hogset A, Berg K. 5-aminolevulinic acid, but not 5-aminolevulinic acid esters, is transported into adenocarcinoma cells by system BETA transporters. Photochemistry and photobiology. 2000; 71(5):640–7. Epub 2000/05/20. PMID: 10818796.

23. Rodriguez L, Batlle A, Di Venosa G, Battah S, Dobbin P, Macrobert AJ, et al. Mechanisms of 5-aminolevulinic acid ester uptake in mammalian cells. British journal of pharmacology. 2006; 147(7):825–33. Epub 2006/01/25. https://doi.org/10.1038/sj.bjp.0706668 PMID: 16432502; PubMed Central PMCID: PMC1751507.

24. Kobuchi H, Moriya K, Ogino T, Fujita H, Inoue K, Shuin T, et al. Mitochondrial localization of ABC transporter ABCG2 and its function in 5-aminolevulinic acid-mediated protoporphyrin IX accumulation. PloS one. 2012; 7(11):e50082. Epub 2012/11/29. https://doi.org/10.1371/journal.pone.0050082 PMID: 23189181; PubMed Central PMCID: PMC3506543.

25. Zhao SG, Chen XF, Wang LG, Yang G, Han DY, Teng L, et al. Increased expression of ABCB6 enhances protoporphyrin IX accumulation and photodynamic effect in human glioma. Annals of surgical oncology. 2013; 20(13):4379–88. Epub 2012/06/13. https://doi.org/10.1245/s10434-011-2201-6 PMID: 22688660.

26. Goodell MA, Rosenzweig M, Kim H, Marks DF, DeMaria M, Paradis G, et al. Dye efflux studies suggest that hematopoietic stem cells expressing low or undetectable levels of CD34 antigen exist in multiple species. Nature medicine. 1997; 3(12):1337–45. Epub 1997/12/13. PMID: 9396603.

27. Zhou S, Schuetz JD, Bunting KD, Colapietro AM, Sampath J, Morris JJ, et al. The ABC transporter Bcrp1/ABCG2 is expressed in a wide variety of stem cells and is a molecular determinant of the side-population phenotype. Nature medicine. 2001; 7(9):1028–34. nm0901-1028 [pii] https://doi.org/10.1038/nm0901-1028 PMID: 11533706.

28. Kondo T, Setoguchi T, Taga T. Persistence of a small subpopulation of cancer stem-like cells in the C6 glioma cell line. Proceedings of the National Academy of Sciences of the United States of America. 2004; 101(3):781–6. Epub 2004/01/09. https://doi.org/10.1073/pnas.0307618100 PMID: 14711994; PubMed Central PMCID: PMC321758.

29. Inoda S, Hirohashi Y, Torigoe T, Morita R, Takahashi A, Asanuma H, et al. Cytotoxic T lymphocytes efficiently recognize human colon cancer stem-like cells. The American journal of pathology. 2011; 178(4):1805–13. Epub 2011/03/26. https://doi.org/10.1016/j.ajpath.2011.01.004 PMID: 21435460; PubMed Central PMCID: PMC3078439.

30. Nokes B, Apel M, Jones C, Brown G, Lang JE. Aminolevulinic acid (ALA): photodynamic detection and potential therapeutic applications. The Journal of surgical research. 2013; 181(2):262–71. Epub 2013/03/21. https://doi.org/10.1016/j.jss.2013.02.002 PMID: 23510551.

31. Natarajan K, Xie Y, Baer MR, Ross DD. Role of breast cancer resistance protein (BCRP/ABCG2) in cancer drug resistance. Biochemical pharmacology. 2012; 83(8):1084–103. Epub 2012/01/18. https://doi.org/10.1016/j.bcp.2012.01.002 PMID: 22248732; PubMed Central PMCID: PMC3307098.

32. Glavinas H, Krajcsi P, Cserepes J, Sarkadi B. The role of ABC transporters in drug resistance, metabolism and toxicity. Current drug delivery. 2004; 1(1):27–42. Epub 2005/11/25. PMID: 16305368.

33. Challen GA, Little MH. A side order of stem cells: the SP phenotype. Stem cells. 2006; 24(1):3–12. Epub 2006/02/02. https://doi.org/10.1634/stemcells.2005-0116 PMID: 16449630.

34. Krishnamurthy P, Schuetz JD. Role of ABCG2/BCRP in biology and medicine. Annual review of pharmacology and toxicology. 2006; 46:381–410. Epub 2006/01/13. https://doi.org/10.1146/annurev.pharmtox.46.120604.141238 PMID: 16402910.

35. Singh RR, Kunkalla K, Qu C, Schlette E, Neelapu SS, Samaniego F, et al. ABCG2 is a direct transcriptional target of hedgehog signaling and involved in stroma-induced drug tolerance in diffuse large B-cell lymphoma. Oncogene. 2011; 30(49):4874–86. Epub 2011/06/01. https://doi.org/10.1038/onc.2011.195 PMID: 21625222; PubMed Central PMCID: PMC3165099.

36. Rosow DE, Liss AS, Strobel O, Fritz S, Bausch D, Valsangkar NP, et al. Sonic Hedgehog in pancreatic cancer: from bench to bedside, then back to the bench. Surgery. 2012; 152(3 Suppl 1):S19–32. Epub

2012/07/10. https://doi.org/10.1016/j.surg.2012.05.030 PMID: 22770959; PubMed Central PMCID: PMC3806061.

37. Catenacci DV, Junttila MR, Karrison T, Bahary N, Horiba MN, Nattam SR, et al. Randomized Phase Ib/II Study of Gemcitabine Plus Placebo or Vismodegib, a Hedgehog Pathway Inhibitor, in Patients With Metastatic Pancreatic Cancer. Journal of clinical oncology: official journal of the American Society of Clinical Oncology. 2015; 33(36):4284–92. Epub 2015/11/04. https://doi.org/10.1200/JCO.2015.62.8719 PMID: 26527777; PubMed Central PMCID: PMC4678179.

38. Wang F, Ma L, Zhang Z, Liu X, Gao H, Zhuang Y, et al. Hedgehog Signaling Regulates Epithelial-Mesenchymal Transition in Pancreatic Cancer Stem-Like Cells. Journal of Cancer. 2016; 7(4):408–17. Epub 2016/02/27. https://doi.org/10.7150/jca.13305 PMID: 26918054; PubMed Central PMCID: PMC4749361.

39. Wang W, Tabu K, Hagiya Y, Sugiyama Y, Kokubu Y, Murota Y, et al. Enhancement of 5-aminolevulinic acid-based fluorescence detection of side population-defined glioma stem cells by iron chelation. Scientific reports. 2017; 7:42070. Epub 2017/02/09. https://doi.org/10.1038/srep42070 PMID: 28169355; PubMed Central PMCID: PMC5294410.

40. Park S, Shimizu C, Shimoyama T, Takeda M, Ando M, Kohno T, et al. Gene expression profiling of ATP-binding cassette (ABC) transporters as a predictor of the pathologic response to neoadjuvant chemotherapy in breast cancer patients. Breast cancer research and treatment. 2006; 99(1):9–17. Epub 2006/06/06. https://doi.org/10.1007/s10549-006-9175-2 PMID: 16752223.

41. Karatas OF, Guzel E, Duz MB, Ittmann M, Ozen M. The role of ATP-binding cassette transporter genes in the progression of prostate cancer. The Prostate. 2016; 76(5):434–44. Epub 2015/12/29. https://doi.org/10.1002/pros.23137 PMID: 26708806.